

# Joint Carrier Frequency Offset, Sampling Time Offset and Channel Estimation for OFDM-OQAM Systems

Ali Baghaki, Benoit Champagne

Department of Electrical and Computer Engineering, McGill University, 3480 University Street  
Montreal, QC, Canada, H3A 0E9

Email: ali.baghaki@mail.mcgill.ca; benoit.champagne@mcgill.ca

**Abstract**—Among the alternative multicarrier modulation techniques to orthogonal frequency division multiplexing (OFDM), a derivative of OFDM based on offset quadrature amplitude modulation (OFDM-OQAM) has been one of the most prominent to alleviate the sensitivity problem of the former to timing and frequency mismatch. In this paper, we propose an improved joint estimation method for carrier frequency offset (CFO), sampling time offset (STO) and channel impulse response (CIR) in OFDM-OQAM systems. The proposed method instruments a data-aided maximum-likelihood (ML) joint estimation of the unknown parameters, as derived under an assumption of Gaussian noise and independent input symbols by splitting the interference into pilot, non-pilot and noise terms. Performance evaluation is carried out through simulations by comparing the proposed method with a highly-cited previous work which considers all the three types of parameters in one development. The improvements in the results indicate the superiority of the proposed joint ML-based estimator.

## I. INTRODUCTION

Due to the several benefits of multicarrier modulation (MCM) over single carrier modulation, the former has been considered as the primary choice in the physical layer implementation of telecommunication systems for quite a long time. Among the MCM family, OFDM-based systems have been largely studied and adopted in many wireless standards [1]. Still, as an alternative and promising form of MCM, OFDM-OQAM has attracted much research attention in recent years, due to its advantages over classical OFDM, including higher spectral efficiency and reduced sensitivity to timing and frequency mismatch [2].

Data-aided CFO, STO and CIR estimation has been a topic of great interest in connection with OFDM-OQAM systems lately. Regarding the CFO and STO synchronization methods, in [3], an ML STO estimator has been derived by using two training symbols as a preamble per burst transmission while in [4], the same preamble and a similar approach have been used for joint CFO and STO synchronization. In [5], by using two identical pilot symbols per burst transmission as preamble, a joint least squares (LS) CFO and STO estimation method has been developed. As well, in [6], a method has been proposed that exploits a polyphase network (PPN) implementation of OFDM-OQAM, a preloading technique and a conjugate-symmetric preamble to jointly estimate the CFO and the STO.

---

This research was jointly funded by InterDigital Canada and the Natural Sciences and Engineering Research Council (NSERC) of Canada, under a CRD Grant.

More recently, in [7], the use of a particular four-column preamble, containing zeros in every other subcarrier and every other symbol time index, has been proposed for the same purpose. Among these techniques, the latter appears to provide better results but lacks the consideration of proper means for the estimation and equalization of fading channels.

In parallel to the CFO and STO synchronization methods, during the past decade, many channel estimation schemes have been proposed for OFDM-OQAM systems. Several of these techniques obtain estimates of the channel or subchannel responses directly in the frequency domain, based on the assumption of nearly flat subchannels [8], [9]. However, in highly frequency-selective channels or when the number of subcarriers is insufficient to cope with the frequency dispersion in fast fading environments, this assumption may not hold and result in severe error floors at medium to high signal-to-noise ratio (SNR) values. In contrast to the above techniques, time-domain channel estimation methods obtain the estimate of the CIR itself and make no assumption on the degree of frequency selectivity of subchannels [10] [11]. Moreover, in time-domain channel estimation, *a priori* information about the channel statistics can be employed to improve the estimation accuracy, as e.g. in [12] for conventional OFDM.

As for the time-domain CIR estimation methods for OFDM-OQAM systems, in [13], the CIR has been estimated by using preamble pilots. Therein, a time-domain channel estimator has been proposed based on the multiple signal classification (MUSIC) and LS algorithms. Later, in [14], a per-subchannel estimator has been developed in which the CIRs on different subcarriers are estimated separately. In a recent paper [11], a general time-domain model for channel estimation in OFDM-OQAM systems has been introduced where frequency domain pilots are used to obtain two estimators, namely the linear-minimum-mean-square-error (LMMSE) and the weighted-least-square (WLS).

Although the aforementioned synchronization and equalization problems have been separately addressed throughout the literature on OFDM-OQAM systems, only a few research papers can be found, e.g. [15], that are devoted to STO, CFO and channel estimation at the same time, let alone a joint estimation approach. In fact, to the best of our knowledge, a joint estimation method for OFDM-OQAM systems, accounting for all the three aforementioned error sources, has not yet been developed. Hence, our focus in this work is to develop and investigate a general method for this purpose. The proposed

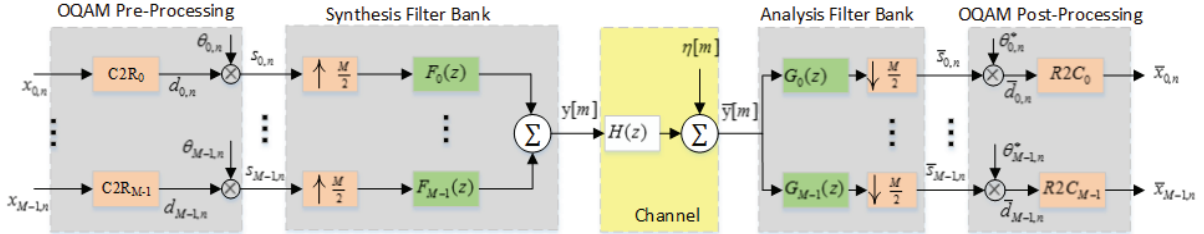


Fig. 1: OFDM-OQAM system model

method relies on a data-aided maximum-likelihood (ML)-based joint estimation of the unknown parameters, as derived by assuming Gaussian noise and independent input symbols, and by splitting the interference into pilot, non-pilot and noise parts. Such a general, joint ML-based method offers many advantages, such as a unified framework for the estimation of multiple parameter using a common preamble/burst structure and the proper treatment of different types of interference in the estimator derivation. Indeed, as it will be seen from the results, the proposed method is capable of significant improvements in parameter estimation accuracy leading to a lower bit error rate (BER) of the compensated (i.e. synchronized and equalized) transceiver system.

The paper is organized as follows. Section 2 is dedicated to reviewing the system model of the OFDM-OQAM system. In Section 3, the proposed joint ML estimator is presented and described in details. The simulation setup and the results are provided in Section 4. Section 5 contains conclusion.

## II. SYSTEM MODEL

The OFDM-OQAM system model, as implemented in this work and commonly used in the literature, see e.g. [16], is illustrated in Fig. 1. The signal at the output of the transmitter synthesis filter bank (SFB) can be described as

$$y[m] = \sum_n \sum_k \underbrace{\theta_{k,n} d_{k,n}}_{s_{k,n}} f_k \left[ m - \frac{nM}{2} \right] e^{-j\frac{2\pi km}{M}} \quad (1)$$

where  $n \in \mathbb{Z}$  and  $k \in \{0, 1, \dots, M-1\}$  are the symbol time index and frequency index, respectively, and  $M$  is the number of subcarriers. In the preprocessing stage, the input symbols  $x_{k,n}$  are complex-to-real converted and multiplied by  $\theta_{k,n} = j^{k+n}$ . The resulting symbols  $s_{k,n}$  are then upsampled by  $M/2$  and passed through their corresponding subband filters,  $f_k[m]$ . The latter are derived from modulation of a common prototype  $p[m]$  via the relationship  $f_k[m] = p[m] e^{j\frac{2\pi k}{M} (m - \frac{Lp-1}{2})}$ .

Upon passing through the channel, the received signal, suffering from CFO, STO, Rayleigh channel effect and additive noise, can be written as

$$\bar{y}[m] = (h[m] * y[m - \tau_0]) e^{\frac{j2\pi\mu_0 m}{M}} + \eta[m] \quad (2)$$

$$= e^{\frac{j2\pi\mu_0 m}{M}} \left( \sum_{l=0}^{Q-1} h[l] y[m - l - \tau_0] \right) + \eta[m] \quad (3)$$

where  $h[l]$  represents the  $l$ th coefficient of the CIR, assumed to be of finite with length  $Q$ ,  $\tau_0$  is the normalized STO with respect to one half of an OFDM-OQAM symbol duration, and  $\mu_0$  is the normalized CFO with respect to the subchannel

frequency spacing, denoted as  $\Delta f$ . Finally,  $\eta[m]$  represents the additive zero-mean white Gaussian noise. It is worth mentioning that, similar to most of the previous works on this subject, the second-order effects, i.e. those of CFO and STO and CIR on one another, have been neglected in this model. It will be seen from the results that these effects are, indeed, negligible.

The OFDM-OQAM symbols at the output of the receiver analysis filter bank (AFB), therefore, will take the form

$$\bar{s}_{k,n} = \sum_{m=-\infty}^{\infty} \bar{y}[m] g_k \left[ m - \frac{nM}{2} \right] e^{j\frac{2\pi km}{M}} + n_{k,n} \quad (4)$$

which by using (2) can be rewritten as

$$\begin{aligned} \bar{s}_{k,n} = & \sum_{m=-\infty}^{\infty} (h[m] * y[m - \tau_0]) e^{\frac{j2\pi\mu_0 m}{M}} g_k \left[ m - \frac{nM}{2} \right] \\ & \times e^{j\frac{2\pi km}{M}} + n_{k,n} \end{aligned} \quad (5)$$

where  $n_{k,n}$  represents the additive noise (i.e. the contribution from  $\eta[m]$ ) passed through the AFB.

## III. PARAMETER ESTIMATION

In this work, an OFDM-OQAM symbol at time  $n$  is defined as the ordered set of  $M$  subband inputs,  $s_{k,n}$ , for  $k \in \{0, 1, \dots, M-1\}$ , entering the SFB (after OQAM pre-processing). To allow for flexibility in the application of the derived method, we consider a general framework for the allocation of pilots. Specifically, within a burst of  $N$  consecutive symbols (e.g., from time  $n = 0$  to  $N-1$ ), a total of  $T$  symbols with time indexes in  $\mathcal{T} \subseteq \{0, \dots, N-1\}$ , are selected for the transmission of pilots over selected subbands from a subset of  $S$  subbands with frequency indexes in  $\mathcal{S} \subseteq \{0, 1, \dots, M-1\}$ .

Starting from (5) and by substituting from (3) and (1), the following expression can be obtained for the output symbols,

$$\bar{s}_{k,n} = \sum_{l=0}^{Q-1} h[l] \lambda_{k,n}(l, \mu_0, \tau_0) + n_{k,n} \quad (6)$$

where

$$n_{k,n} = \sum_{m=-\infty}^{\infty} \eta[m] g_k \left[ m - \frac{nM}{2} \right] e^{j\frac{2\pi km}{M}} \quad (7)$$

$$\lambda_{k,n}(l, \mu_0, \tau_0) = \sum_{k'=0}^{M-1} \sum_{n'=-\infty}^{\infty} s_{k',n'} \gamma_{k,n'}^{k',n'}(l, \mu_0, \tau_0) \quad (8)$$

In turn, we have

$$\begin{aligned} \gamma_{k,n}^{k',n'}(l, \mu_0, \tau_0) = & \\ \sum_{m=-\infty}^{\infty} f_{k'}[m-l-\tau_0 - \frac{n'M}{2}] g_k[m - \frac{nM}{2}] & \quad (9) \\ \times \exp\left(\frac{-j2\pi}{M}(k'(m-l-\tau_0) - \mu_0 m - km)\right) \end{aligned}$$

The term  $\gamma_{k,n}^{k',n'}(l, \mu_0, \tau_0)$  characterizes the level of the ‘intrinsic interference’ of the  $n'$ th input sample from the  $k'$ th subband,  $s_{k',n'}$ , on the  $n$ th output sample from the  $k$ th subband,  $\bar{s}_{k,n}$ , through the  $l$ th path of the channel  $h[l]$  in the presence of CFO,  $\mu_0$ , and STO,  $\tau_0$ . We note that due to the finite length of the subband filter  $f_k[m]$ , the summation in (9) is in fact performed over a finite range. It is worth mentioning that in previous works, e.g. [7] and [15], it has been assumed that due to the finite duration of the filter bank and the fact that CFO values are often small, the CFO term  $e^{j2\pi\mu_0 m/M}$  remains constant. Under this assumption, hence, this term could be taken out of the summation over  $m$  in (9) and as a result, the CFO contribution to  $\gamma_{k,n}^{k',n'}(l, \mu_0, \tau_0)$  would be negligible when  $n' \neq n$  and  $k' \neq k$ . However, in this work, the intention is to avoid such a simplification to achieve an ML solution that is more accurate than the simplified methods.

Next, focusing on the pilot symbols, i.e.  $n \in \mathcal{T}$  and  $k \in \mathcal{S}$ , and by replacing  $s_{k',n'}$  by  $p_{k',n'}$  in (8) for the sent pilot symbols, we define

$$\bar{\lambda}_{k,n}(l, \mu_0, \tau_0) = \sum_{k' \in \mathcal{S}} \sum_{n' \in \mathcal{T}} p_{k',n'} \gamma_{k,n}^{k',n'}(l, \mu_0, \tau_0) \quad (10)$$

Consequently, (6) is changed to the following form

$$\bar{s}_{k,n} = \sum_{l=0}^{Q-1} h[l] \bar{\lambda}_{k,n}(l, \mu_0, \tau_0) + w_{k,n} + n_{k,n} \quad (11)$$

where

$$w_{k,n} = \sum_{l=0}^{Q-1} \sum_{k' \notin \mathcal{S}} \sum_{n' \notin \mathcal{T}} s_{k',n'} \gamma_{k,n}^{k',n'}(l, \mu_0, \tau_0) h[l] \quad (12)$$

In (12),  $w_{k,n}$  represents the interference contribution from all non-pilot symbols surrounding the desired pilot to the corresponding received pilot, which is called ‘data-interference’.

Assuming independent and identically distributed data symbols with zero mean and variance of  $\sigma_s^2$ , similar to [17], it can be shown that the interference terms,  $\{w_{k,n}\}$ , can be approximated as independent Gaussian random variables with zero mean and variance of

$$\sigma_w^2 = E\{|w_{k,n}|^2\} = \sigma_s^2 \sum_{k' \notin \mathcal{S}} \sum_{n' \notin \mathcal{T}} |\Gamma_{k,n}^{k',n'}(\mu_0, \tau_0)|^2 \quad (13)$$

where

$$\Gamma_{k,n}^{k',n'}(\mu_0, \tau_0) = \sum_{l=0}^{Q-1} \gamma_{k,n}^{k',n'}(l, \mu_0, \tau_0) h[l]$$

Introducing  $v_{k,n} = w_{k,n} + n_{k,n}$  and assuming that the data and the additive noise are independent, it follows that  $v_{k,n}$  are independent Gaussian random variables with variance  $\sigma_v^2 = \sigma_w^2 + \sigma_n^2$ .

Next, by substituting  $v_{k,n}$  in (11) and letting

$$\mathbf{h} = [h[0], h[1], \dots, h[Q-1]]^T$$

$$\boldsymbol{\lambda}_{k,n}(\mu_0, \tau_0) = [\bar{\lambda}_{k,n}(0, \mu_0), \bar{\lambda}_{k,n}(1, \mu_0), \dots, \bar{\lambda}_{k,n}(Q-1, \mu_0)]$$

we will have

$$\bar{s}_{k,n} = \boldsymbol{\lambda}_{k,n}(\mu_0, \tau_0) \mathbf{h} + v_{k,n} \quad (14)$$

By stacking  $\boldsymbol{\lambda}_{k,n}(\mu_0, \tau_0)$ ,  $\bar{s}_{k,n}$  and  $v_{k,n}$  over the time index  $n \in \mathcal{T}$  for each  $k$ , and then over the frequency index  $k \in \mathcal{S}$ , we define the corresponding matrix and vectors  $\boldsymbol{\Lambda}(\mu_0, \tau_0)$ ,  $\bar{\mathbf{S}}$  and  $\mathbf{V}$ . In terms of these new quantities, (14) now takes the following matrix-vector form,

$$\bar{\mathbf{S}} = \boldsymbol{\Lambda}(\mu_0, \tau_0) \mathbf{h} + \mathbf{V} \quad (15)$$

As a result of the AWGN assumption and the ensuing approximations on the interference  $w_{k,n}$ ,  $\mathbf{V}$  will be a complex circular Gaussian random vector with zero mean and diagonal covariance matrix  $\mathbf{C}_V = E[\mathbf{V}\mathbf{V}^H] = \sigma_v^2 \mathbf{I}$ . Similarly, for given values of  $\mu_0$ ,  $\tau_0$  and  $\mathbf{h}$ , the observation vector  $\bar{\mathbf{S}}$  is also complex circular Gaussian with mean  $\boldsymbol{\Lambda}(\mu_0, \tau_0) \mathbf{h}$  and covariance  $\mathbf{C}_{\bar{\mathbf{S}}} = \sigma_v^2 \mathbf{I}$ . Hence, the probability density function (PDF) of  $\bar{\mathbf{S}}$  can be presented as

$$\begin{aligned} f(\bar{\mathbf{S}}; \mu_0, \tau_0, \mathbf{h}) = & \frac{1}{\pi^{N_p} \det(\mathbf{C}_{\bar{\mathbf{S}}})} \\ \times \exp[-(\bar{\mathbf{S}} - \boldsymbol{\Lambda}(\mu_0, \tau_0) \mathbf{h})^H \mathbf{C}_{\bar{\mathbf{S}}}^{-1} (\bar{\mathbf{S}} - \boldsymbol{\Lambda}(\mu_0, \tau_0) \mathbf{h})] \end{aligned} \quad (16)$$

where  $N_p = TS$  is the number of pilots. Thus, the log-likelihood function (LLF) is written, up to a constant, as

$$\begin{aligned} \mathcal{L}(\bar{\mathbf{S}}; \mu_0, \tau_0, \mathbf{h}) = & \log(f(\bar{\mathbf{S}}; \mu_0, \tau_0, \mathbf{h})) \\ = & -\frac{1}{\sigma_v^2} [\bar{\mathbf{S}} - \boldsymbol{\Lambda}(\mu_0, \tau_0) \mathbf{h}]^H [\bar{\mathbf{S}} - \boldsymbol{\Lambda}(\mu_0, \tau_0) \mathbf{h}] \end{aligned} \quad (17)$$

The joint ML estimators of the CFO, CIR and STO can be obtained by maximizing the derived LLF with respect to the parameters  $\mu_0$ ,  $\tau_0$  and  $\mathbf{h}$ . By fixing  $\mu_0$  and  $\tau_0$  and varying  $\mathbf{h}$  in  $\mathbb{C}^Q$ , the LLF achieves its maximum at

$$\hat{\mathbf{h}}(\mu_0, \tau_0) = \boldsymbol{\Lambda}(\mu_0, \tau_0)^\dagger \bar{\mathbf{S}} \quad (18)$$

where  $\boldsymbol{\Lambda}(\mu_0, \tau_0)^\dagger = (\boldsymbol{\Lambda}(\mu_0, \tau_0)^H \boldsymbol{\Lambda}(\mu_0, \tau_0))^{-1} \boldsymbol{\Lambda}(\mu_0, \tau_0)^H$  is the pseudo-inverse of  $\boldsymbol{\Lambda}(\mu_0, \tau_0)$ . By substituting (18) into the LLF we can obtain the CFO and STO estimates using a 2-dimensional search according to

$$(\hat{\mu}, \hat{\tau}) = \arg \max_{\mu_0, \tau_0} \mathcal{L}(\bar{\mathbf{S}}; \mu_0, \tau_0, \hat{\mathbf{h}}) \quad (19)$$

Finally, the ML estimate of the CIR can be obtained by substituting the estimates  $(\hat{\mu}, \hat{\tau})$ , resulting in

$$\hat{\mathbf{h}} = \tilde{\mathbf{h}}(\hat{\mu}, \hat{\tau}) = \boldsymbol{\Lambda}(\hat{\mu}, \hat{\tau})^\dagger \bar{\mathbf{S}} \quad (20)$$

In our implementation of the above ML approach, certain simplifications are made to (10) in order to reduce the computational complexity; however, these cannot be described in details due to space limitations.

Fig. 2 illustrates the block diagram of the OFDM-OQAM receiver as implemented in the proposed method for estimation and compensation of CFO, STO and CIR. First, after passing through the AFB, the received symbols are used to obtain the ML estimates of the CFO, STO and CIR. The CFO and STO estimates are then fed back to correct the symbols at the input of the receiver. Next, the STO-CFO corrected symbols pass through the AFB again where, this time, a single-tap per subcarrier equalization is performed based on the DFT of the estimated CIR. The final received symbols are obtained by undergoing the OQAM post-processing stage.

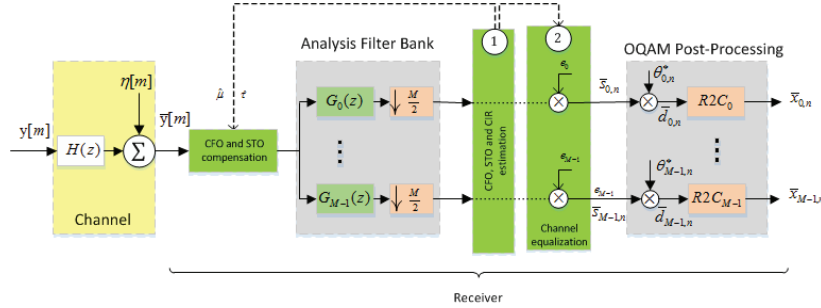


Fig. 2: Block diagram of the OFDM-OQAM receiver with ML-based compensation

#### IV. PERFORMANCE EVALUATION

In this section, the proposed method is compared with the one in [15], the only research paper found by the authors that has considered all three parameters of concern, namely, STO, CFO and CIR. However, in [15], this has been achieved by using different ideas for different parameters rather than developing a joint method from a unified, general criterion.

##### A. Simulation Setup

To compare the two methods, two different distributions of pilots are considered in the implementation of the proposed method. In the first distribution, the pilots are scattered within each burst as mentioned in [15]. Specifically, the size of the transmitted bursts in time and frequency are according to DL-PUSC configuration as illustrated in Figs. 4 and 5 of this reference, with  $M = 256$  subcarriers and  $N = 12$  OQAM subsymbols (6 OQAM symbols before preprocessing) in total. The other distribution, which also uses  $M = 256$  subcarriers, adopts a full preamble of  $T = 12$  pilot tones, followed by  $N - T = 72$  data symbols. The consideration of these two different distributions of pilot tones is useful to assess the performance of different transmission modes. Moreover, in order to have a fair comparison, all the three implementations share the same bit rate.

The prototype filter of the transceiver system is obtained using the frequency sampling technique with overlap factor  $K = 4$  as described in [16] and used in [15]. The data are modulated to a 4-QAM constellation. The input sampling frequency is  $F_s = 43.75\text{kHz}$  corresponding to a channel bandwidth of  $MF_s = 11.2\text{MHz}$ . To obtain BER that are more representative of a practical digital communications system, a punctured convolutional channel coding scheme is applied to the information sequence with the overall rate of  $3/4$  by using constraint length  $\kappa = 7$ , function generators  $g_1 = [133]$ ,  $g_2 = [171]$  and the puncture pattern vector  $[110110]$ . A frequency selective wireless channel is used with  $Q = 8$  randomly generated coefficients  $h[l]$  based on the ITU-Vehicular A channel guidelines [18]. The channel is assumed constant during the transmission of a burst but changes over different transmissions. During each transmission, the STO and CFO are chosen randomly within the intervals  $[-\frac{\Delta T}{4}, \frac{\Delta T}{4}]$  and  $[-\frac{\Delta f}{4}, \frac{\Delta f}{4}]$  where  $\Delta T = MT_s$ . The root mean squared error (RMSE) and BER results are obtained by running 500 independent Monte-Carlo simulations. Regarding the implementation results of [15], we follow the estimation and equalization algorithms and structure precisely as described in the paper. This method is referred to as 'Stitz' in Figs. 3–6.

##### B. Results

Fig. 3 compares the proposed method with [15] in terms of RMSE of CFO. The estimation is jointly performed in the presence of other sources of error, namely, a fixed STO of 10% with respect to one half of an OQAM symbol duration and Rayleigh channel as described earlier. The figure indicates that the proposed method not only outperforms the other method as implemented with a preamble of full  $256 \times 12$  pilot tones, but also, is capable of significant improvement when adopting the burst structure of DL-PUSC.

Comparison of the two methods in terms of RMSE of STO is depicted in Fig. 4, where a fixed CFO of 5% and the multi-path channel are used. The superior performance of the proposed method implemented in both configurations can be seen in the figure. Again, the best result belongs to the one based on a full grid of pilot tones followed by the data; although, the proposed method remarkably reduces the estimation error with the same burst structure as in [15]. The flattening of the graphs at the end is due to the limited search resolution of the implementation compared to the fractional delay that could occur. This can be overcome by adding a fine STO estimation with a more accurate search grid as a second step.

In Fig. 5, the RMSE of CIR, in the presence of fixed CFO and STO, is depicted for the three implementations. Similar to the previous Figs., the proposed method achieves a lower estimation error in both configurations. Finally, the coded BER performance of the methods, after estimation and compensation, are compared in Fig. 6. The figure indicates that, in both configurations, the proposed method is capable of a significant decrease in BER of the system especially at high input  $E_b/N_0$ .

After applying the aforementioned simplifications in Section 3, the proposed method achieves about the same order of computational complexity as [15], in terms of the running time.

#### V. CONCLUSION

A new general data-aided ML-based joint estimation method for OFDM-OQAM systems has been developed and evaluated. The CFO, the STO, and the CIR effects have been jointly estimated and compensated. The comparison has been made with a highly-cited method among the few research papers to consider all the three parameters at the same time. The results have shown the significant improvement that the proposed method offers in both transmission modes, i.e., as scattered pilots in data and as a full preamble of pilot tones followed by the data.

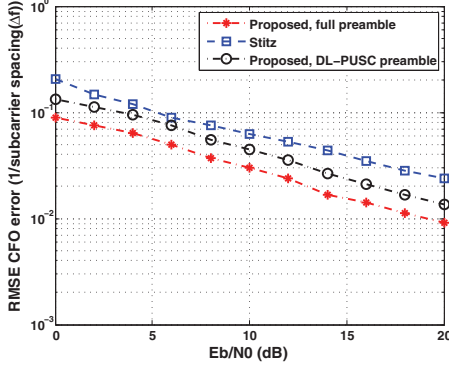


Fig. 3: Comparative RMSE error of CFO estimation versus input  $E_b/N_0$  with STO = 10% and Rayleigh channel.

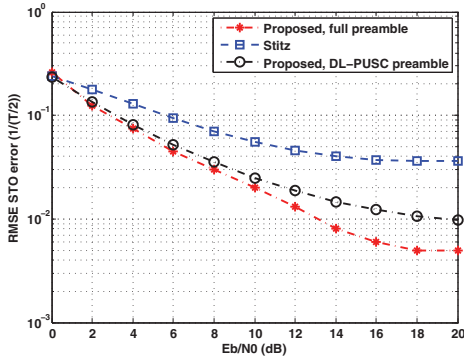


Fig. 4: Comparative RMSE error of STO estimation versus input  $E_b/N_0$  with CFO = 5% and Rayleigh channel.

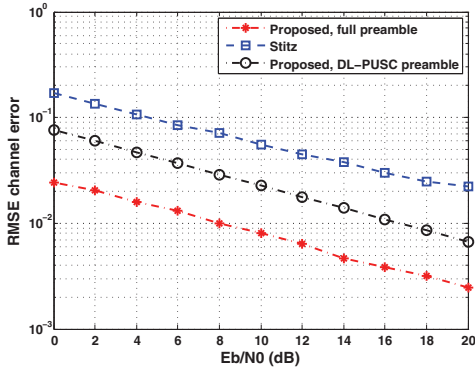


Fig. 5: Comparative RMSE error of channel estimation versus input  $E_b/N_0$  with CFO = 5% and STO = 10%.

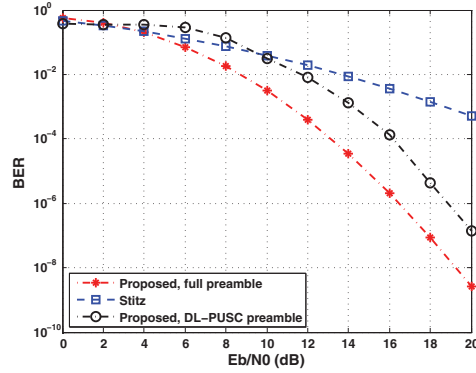


Fig. 6: Comparative coded BER versus input  $E_b/N_0$  in the presence of CFO, STO and channel estimation.

*Int. Conf. Communications (ICC)*, June 2009, pp. 1–5.

- [4] T. Fusco, A. Petrella, and M. Tanda, “Joint symbol timing and CFO estimation for OFDM/OQAM systems in multipath channels,” *EURASIP J. Advances Signal Process.*, Jan., 2010.
- [5] T. Fusco, A. Petrella, and M. Tanda, “Data-aided symbol timing and CFO synchronization for filter bank multicarrier systems,” *IEEE Trans. Wireless Commun.*, vol. 8, no. 5, pp. 2705–2715, May, 2009.
- [6] D. Mattera and M. Tanda, “Data-aided synchronization for OFDM/OQAM systems,” *Signal Process.*, vol. 92, pp. 2284 – 2292, Sept., 2012.
- [7] C. Thein, M. Fuhrwerk, and J. Peissig, “Frequency-domain processing for synchronization and channel estimation in OQAM-OFDM systems,” in *Proc. IEEE 14th SPAWC*, June 2013, pp. 634–638.
- [8] C. Lélé, J.-P. Javaudin, R. Legoussé, A. Skrzypczak, and P. Siohan, “Channel estimation methods for preamble-based OFDM/OQAM modulations,” in *Proc. Eur. Wireless Conf.*, Mar. 2007, pp. 59–64.
- [9] S. Hu, G. Wu, and S. Li, “Preamble design and iterative channel estimation for OFDM/Offset QAM System,” *J. Networks*, vol. 4, no. 10, pp. 1050–1057, Dec., 2009.
- [10] E. Kofidis, “Preamble-based channel estimation in OFDM/OQAM systems: A time-domain approach,” 2013, Available: <http://arxiv.org/abs/1306.2581>.
- [11] D. Kong, D. Qu, and T. Jiang, “Time domain channel estimation for OQAM-OFDM systems: Algorithms and performance bounds,” *IEEE Trans. Signal Process.*, vol. 62, no. 2, pp. 322–330, Jan., 2014.
- [12] J.-J. van de Beek, O. Edfors, M. Sandell, S. K. Wilson, and P. O. Börjesson, “On channel estimation in OFDM systems,” in *Proc. IEEE 45th Conf. Veh. Technol.*, Jul. 1995, pp. 815–819.
- [13] G. Garbo, S. Mangione, and V. Maniscalco, “MUSIC-LS modal channel estimation for an OFDM-OQAM system,” in *Proc. 2nd Int. Conf. Signal Process. Commun. Syst. (ICSPCS)*, Dec 2008, pp. 1–8.
- [14] L. G. Baltar, M. Newinger, and J. A. Nossek, “Structured subchannel impulse response estimation for filter bank based multicarrier systems,” in *Proc. ISWCS*, Aug. 2012, pp. 191–195.
- [15] T. H. Stitz, T. Ihälainen, A. Virolainen, and M. Renfors, “Pilot-based synchronization and equalization in filter bank multicarrier communications,” *EURASIP J. Advances Signal Process.*, pp. 1–18, Feb., 2010.
- [16] A. Virolainen, T. Ihälainen, T. H. Stitz, M. Renfors, and M. Bellanger, “Prototype filter design for filter bank based multicarrier transmission,” in *Proc. 17th Eur. Signal Process. Conf. (EUSIPCO)*, Glasgow, Scotland, Aug. 2009, vol. 17, pp. 1359–1363.
- [17] S. Rahimi and B. Champagne, “Joint channel and frequency offset estimation for oversampled perfect reconstruction filter bank transceivers,” *IEEE Trans. Commun.*, vol. 62, no. 6, pp. 2009–2021, June, 2014.
- [18] “ITU-R M. Guidelines for evaluation of radio transmission technologies for IMT-2000 1225,” 1997.

## REFERENCES

- [1] L. Hanzo, Y. Akhtman, L. Wang, and M. Jiang, *OFDM for Wireless Multimedia Communications*, John Wiley, Hoboken, NJ, USA, 2011.
- [2] B. Farhang-Boroujeny, “OFDM versus filterbank multicarrier,” *IEEE Signal Process. Mag.*, vol. 28, pp. 92–112, May, 2011.
- [3] T. Fusco, A. Petrella, and M. Tanda, “Data-aided symbol timing estimation for multiple-access OFDM/OQAM systems,” in *Proc. IEEE*